Title	A rigorous analytical model for shrinkage cracking of reinforced concrete
Author(s)	Ng, PL; Kwan, AKH
Citation	Magazine of Concrete Research, 2017, v. 69 n. 3, p. 120-133
Issued Date	2017
URL	http://hdl.handle.net/10722/250280
Rights	Permission is granted by ICE Publishing to print one copy for personal use. Any other use of these PDF files is subject to reprint fees; This work is licensed under a Creative Commons Attribution-NonCommercial-NoDerivatives 4.0 International License.

Magazine of Concrete Research
Volume 69 Issue 3

A rigorous analytical model for shrinkage cracking of reinforced concrete
Ng and Kwan

Magazine of Concrete Research, 2017, **69**(3), 120–133
http://dx.doi.org/10.1680/jmacr.16.00042
Paper 1600042
Received 15/01/2016; revised 02/10/2016; accepted 05/10/2016
Published online ahead of print 15/11/2016
Keywords: cracks & cracking/shrinkage/structural analysis

ice Institution of Civil Engineers
publishing

A rigorous analytical model for shrinkage cracking of reinforced concrete

Pui-Lam Ng
Department of Civil Engineering, The University of Hong Kong, Pokfulam, Hong Kong, China; Faculty of Civil Engineering, Vilnius Gediminas Technical University, Vilnius, Lithuania (corresponding author: irdngpl@gmail.com)

Albert Kwok-Hung Kwan
Department of Civil Engineering, The University of Hong Kong, Pokfulam, Hong Kong, China

Concrete shrinks as it dries. If its shrinkage movement is restrained, it can crack, causing serviceability and durability problems. To ensure satisfactory performance of a reinforced concrete (RC) structure, the shrinkage crack widths are generally controlled to within acceptable limits by providing steel reinforcement for crack control. However, due to unavoidable empiricism, the design guidelines given in the various design codes for computing the amount of crack-control steel are rather inconsistent. Moreover, the various existing models for prediction of crack widths do not agree with each other, indicating that the shrinkage cracking phenomenon is still far from fully understood. With the aim of resolving this problem, a rigorous analytical model for shrinkage cracking of RC is presented. The governing equations are first derived purely based on the mechanics of the steel bar–concrete interaction. The governing equations are then solved analytically without making any unjustified assumptions. Finally, the analytical model is validated through analysis of experimental results from the literature.

Notation

A_c	concrete section area
A_s	steel area
E_c	elastic modulus of concrete
E_c^*	effective elastic modulus of concrete
E_s	elastic modulus of steel
f_b	average bond strength
f_{cc}	cylinder compressive strength of concrete
f_{ct}	tensile strength of concrete
k_b	bond stiffness
L	length of concrete member between restraints
l	bond force transfer length
l_{max}	maximum crack spacing
l_{min}	minimum crack spacing in BS 8007 (BSI, 1987)
l^*	upper limit of bond force transfer length
l_t	bond force transfer length
l_t^*	upper limit of bond force transfer length in the model of Häußler-Combe and Hartig (2012)
l_0	minimum crack spacing in the model of Nejadi and Gilbert (2004)
m	modular ratio
m^*	effective modular ratio
n	number of steel bars
n_{cr}	number of cracks
n_l	number of transfer lengths
s_b	bond slip
s_r	crack spacing
s_1	bond slip at peak bond stress
u_c	displacement of concrete
u_s	displacement of steel
w	crack width
w_{max}	maximum crack width
x	distance from crack
β_t	constant empirical factor describing the shape of the steel stress distribution along the transfer length
γ	proportionality constant
Δu	change in member length due to support movement
$\Delta\sigma_s$	change in steel stress between the two ends of transfer length
ε	effective strain
ε_{cE}	imposed strain
ε_{cm}	mean strain of concrete
ε_{cs}	shrinkage strain
ε_{cs}^*	ultimate concrete shrinkage strain
ε_{sm}	mean strain of steel
ξ	maximum bond slip
ρ	steel ratio
σ_{av}	average stress in uncracked concrete
σ_c	concrete stress
σ_{cm}	mean concrete stress
σ_{c1}	concrete stress at distance of l_0 from the crack
σ_{c1}^*	final concrete stress at distance of l_0 from the crack
σ_s	steel stress
σ_{sm}	mean steel stress
σ_{sr}	maximum steel stress
σ_{s1}	steel stress at distance of l_0 from the crack

σ_{s2}	steel stress at crack
σ_{s2}^*	final steel stress at crack
τ_b	bond stress
τ_m	mean bond stress
τ_p	peak bond stress
ϕ	steel bar diameter
ϕ_c	creep coefficient
ϕ_c^*	final creep coefficient

Introduction

The shrinkage of concrete after hardening is to some extent unavoidable. In a long reinforced concrete (RC) structure restrained at the ends from longitudinal movement, such as a podium floor deck connected at each end to a rigid core wall, the shrinkage-induced tensile stress could exceed the tensile strength of concrete, thus resulting in the formation of shrinkage cracks. Shrinkage cracks are typically through cracks (i.e. cracks going through the whole thickness of the concrete section) that allow not only the ingress of moisture and deleterious chemicals to reach the steel reinforcing bars, but also create paths of water leakage from the upper floor to the lower floor. Such shrinkage cracking could pose serviceability and durability problems. To ensure satisfactory performance of RC structures, the shrinkage crack widths must be controlled to within acceptable limits (Castel and Gilbert, 2014; Hughes, 1971a, 1971b). However, to do so, the crack widths need to be evaluated in the first place.

Shrinkage cracking may be alleviated or controlled by a number of measures (Kwan *et al*., 2002, 2003). Basically, these include the provision of movement joints, the provision of late-cast strips, the use of high-performance concrete with better dimensional stability, the addition of expanding or shrinkage reducing agents to the concrete mix, and the provision of crack-control steel reinforcement. The provision of crack-control steel, which does not affect construction scheduling, is the most commonly adopted among these measures. However, the relationships between the concrete tensile strength, the ultimate shrinkage strain, the crack-control steel provided and the resulting crack spacings and crack widths are still not well understood. Fairly high levels of empiricism and conservatism have been adopted in various design guides and codes such as British standard BS 8007 (BSI, 1987). As a result, the amount of crack-control steel to be provided is often quite large.

After cracking, the shrinking concrete tends to move away from the cracks and this tendency is opposed by the crack-control steel through the steel bar–concrete bond. It limits the shrinkage movement of the concrete and thus reduces the crack widths to smaller values. Although at the cracks the concrete tensile stresses are relieved to zero, the bond action would still induce tensile stresses in the concrete, which are generally larger at greater distance from the nearest crack. As the shrinkage further increases, the tensile stresses in between two existing cracks increase and eventually can become large enough to cause the formation of a new crack. In general, the provision of more crack-control steel would lead to the formation of more cracks with smaller crack widths. On the other hand, the shrinkage movement of the concrete pulls the crack-control steel away from the cracks through the steel bar–concrete bond. As a result, the crack-control steel would be subjected to much higher tensile stresses at the cracks than at other locations. Figure 1 illustrates the spatial distributions of concrete, steel and bond stresses across a shrinkage crack.

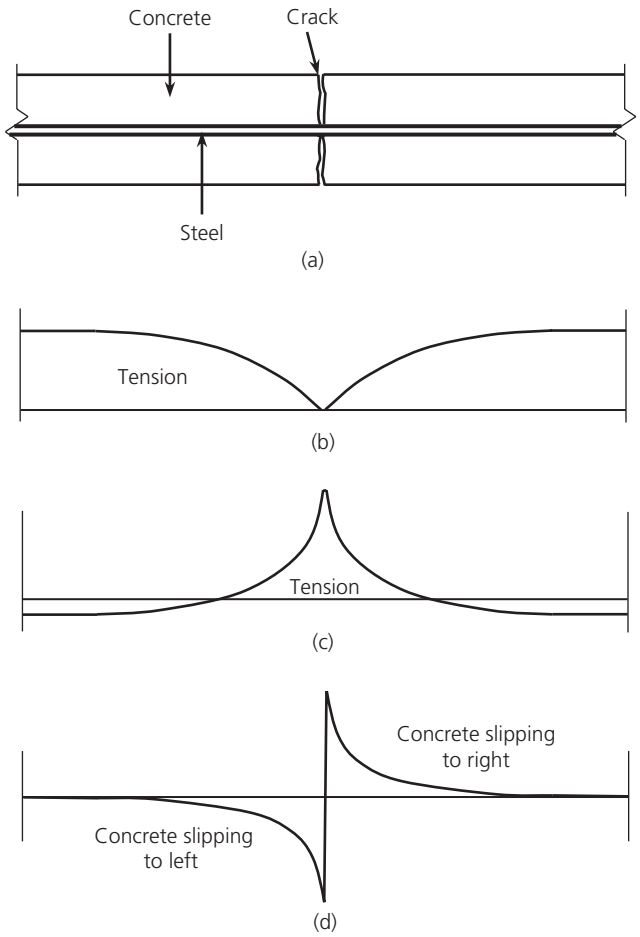

Figure 1. Stress distributions across a shrinkage crack: (a) cracked RC member; (b) concrete stress; (c) steel stress; (d) bond stress

Some simple formulas for the determination of the crack spacing and crack width are given in BS 8007 (BSI, 1987). These formulas are based on the assumption that the bond stress is uniform near the cracks. While such an assumption is rather empirical and might not be justified, it has the advantage of being simple to use. Gilbert (1992, 2001) developed an analytical model for evaluating shrinkage cracking in fully restrained concrete members. It is based on the assumption that the concrete, steel and bond stresses would vary along the

length only within a certain distance from the crack. This distance is evaluated using an empirical expression in terms of only the crack-control steel ratio and diameter. However, in some cases, the computed crack spacing could be unreasonably large or small. Gilbert (2003) and Nejadi and Gilbert (2004) later improved this model by modifying the previous formulas. More recently, Häußler-Combe and Hartig (2012) proposed another analytical model based on certain empirical coefficients for evaluating the crack spacing and crack width. Their model was validated using the experimental results reported by Nejadi and Gilbert (2004).

Apart from these analytical models, finite-element models have also been developed to analyse the shrinkage movement and cracking of RC structures (Jurkiewiez *et al*., 1999; Kwan and Ng, 2009; Liu *et al*., 2006). In the finite-element models, time step analyses were applied to evaluate the spatial and temporal variations of the bond, concrete and steel stresses. Theoretically, the finite-element models should be more rigorous and generally applicable. However, with the bond slip at the steel bar–concrete interface ignored, the concrete and steel bars modelled as an integrated continuum and the cracks modelled as smeared cracks rather than as discrete cracks, these finite-element models are not capable of giving the crack spacing and crack width in the computed results (Ma and Kwan, 2015). For these reasons, the evaluation of the amount of crack-control steel needed and the resulting crack spacing and crack width still cannot be carried out using the finite-element method.

To rationalise the design of steel for the control of shrinkage cracking, the relationships between the material properties, the ratio and diameter of the crack-control steel, crack spacing and crack width need to be established. A rigorous analytical model for shrinkage cracking of RC is developed in this paper based on a set of governing differential equations. By solving the governing differential equations analytically, closed-form solutions are obtained, from which the effects of various structural parameters on the crack spacing and crack width may be evaluated algebraically and the crack-control steel needed may be evaluated directly.

Shrinkage and creep of concrete

As shrinkage takes place and tensile stresses are induced in concrete due to movement restraint, creep also occurs, thus relieving parts of the shrinkage-induced tensile stresses through relaxation (Kwan and Ng, 2015). Both shrinkage and creep are time-dependent, as explained in the following section.

There are two main types of concrete shrinkage – autogenous shrinkage and drying shrinkage (Neville, 2011). Autogenous shrinkage is caused by self-desiccation, whereas drying shrinkage is caused by loss of water due to evaporation. Generally, autogenous shrinkage is fairly small compared with drying shrinkage. Since the loss of water over time depends on the permeability of the concrete, the size of the concrete member and the environmental conditions, the rate of drying shrinkage is also dependent on these factors (Kwan *et al*., 2010). On the other hand, there are two dominant mechanisms of concrete creep. The first mechanism is viscous sliding of the C–S–H (calcium silicate hydrate) gel particles (Neville, 1958; Vandamme and Ulm, 2009). The second mechanism is the internal movement of adsorbed or intra-crystalline water, which is believed to be caused mainly by changes in the hygral equilibrium within the pore structure of the gel inside concrete (Neville, 1955; Powers, 1968). As for drying shrinkage, the rate of creep is also dependent on the permeability of the concrete, the size of the concrete member, and the environmental conditions.

However, it takes many months to measure the shrinkage and creep of a particular concrete. Therefore, in usual practice, the shrinkage strain is just evaluated using the shrinkage coefficient given in design codes and the creep effect is taken into account by changing the elastic modulus to the long-term elastic modulus, which may be evaluated using the creep coefficient given in design codes (Gilbert and Ranzi, 2011).

Bond stress–slip constitutive model

At the steel bar–concrete interface, bond slip occurs and bond stresses are developed. The bond stiffness of the interface affects the effectiveness of the crack-control steel and should thus be properly accounted for. For the bond stress–slip relation, CEB-FIP Model Code 1990 (hereafter referred to as MC-90) (CEB, 1993) gives the bond stress–slip curve shown in Figure 2. According to MC-90, if ribbed steel bars are used (plain round bars are rarely used nowadays because of inferior bond), the bond slip at which peak bond stress would be developed is 0·6 mm, regardless of whether the concrete is

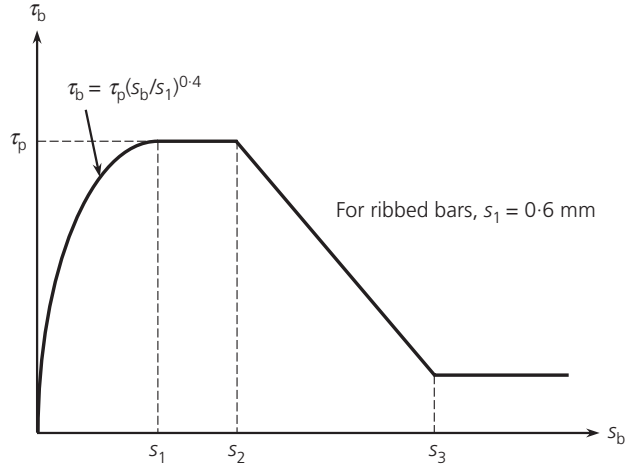

Figure 2. Bond stress–slip curve given in MC-90 (CEB, 1993)

unconfined or confined. Such a bond slip value of 0·6 mm is actually quite large. As the crack width is twice the bond slip, and the allowable crack width is generally not larger than 0·3 mm, the bond slip at the serviceability limit state has to be controlled to within $0{\cdot}5 \times 0{\cdot}3$ mm = 0·15 mm. Basically, before the peak bond stress is developed, the bond stress is an increasing function of the bond slip. Herein, for simplicity, the bond stress is assumed to be proportional to the bond slip and the bond stiffness k_b is taken to be the mean secant stiffness, as evaluated below. As per MC-90, at bond slip s_b not larger than that giving the peak bond stress, the bond stress τ_b is related to the peak bond stress τ_p by

$$1. \quad \tau_b = \tau_p (s_b/s_1)^{0{\cdot}4}$$

where s_1 is the bond slip at peak bond stress. The secant bond stiffness is equal to τ_b/s_b and the mean secant stiffness within the range of bond slip from $0{\cdot}02s_b$ to s_b may be evaluated from Equation 2 (the bond stiffness in MC-90 is unreasonably or even infinitely large at very small bond slip and therefore is not included in the evaluation).

$$2. \quad k_b = \frac{1}{0{\cdot}98 s_b} \int_{0{\cdot}02 s_b}^{s_b} \tau_p \frac{(s_b/s_1)^{0{\cdot}4}}{s_b} \mathrm{d}s_b = 2{\cdot}0(\tau_p/s_b)(s_b/s_1)^{0{\cdot}4}$$

Regarding the peak bond stress τ_p, MC-90 suggests that it may be taken as $2{\cdot}0(f_{cc})^{0{\cdot}5}$ for unconfined concrete or as $2{\cdot}5(f_{cc})^{0{\cdot}5}$ for confined concrete, where f_{cc} is the cylinder compressive strength of the concrete.

Existing methods of shrinkage cracking analysis

Three common methodologies for shrinkage cracking analysis – the method given in BS 8007 (BSI, 1987), the model developed by Nejadi and Gilbert (2004) and the model developed by Häußler-Combe and Hartig (2012) – are highlighted in this section.

The BS 8007 method

At a crack, the concrete stress is zero. Assuming uniform bond stress near the crack, the concrete stress σ_c at a distance l from the crack is equal to

$$3. \quad \sigma_c = \frac{l(n\pi\phi) f_b}{A_c} = l\left(\frac{4\rho}{\phi}\right) f_b$$

where n is the number of steel bars, ϕ is the steel bar diameter, ρ is the steel ratio, f_b is the average bond strength and A_c is the concrete section area. The concrete would crack again at a minimum distance from the existing crack of l_{min}, where σ_c reaches the tensile strength of concrete f_{ct}. Based on this condition, the minimum crack spacing l_{min} may be obtained as

$$4. \quad l_{min} = \left(\frac{\phi}{4\rho}\right)\left(\frac{f_{ct}}{f_b}\right)$$

Between two existing cracks, the concrete stress increases from zero at one crack to a maximum value at mid-distance between the two cracks and then decreases to zero at the other crack. If the distance between the two existing cracks is longer than $2l_{min}$, the maximum concrete stress would be higher than the tensile strength and a new crack would be formed between the two existing cracks. Hence, the maximum crack spacing l_{max} may be taken as

$$5. \quad l_{max} = 2l_{min} = \left(\frac{\phi}{2\rho}\right)\left(\frac{f_{ct}}{f_b}\right)$$

From the above, the maximum crack width w_{max} is derived as

$$6. \quad w_{max} = l_{max}\varepsilon$$

where ε is the effective strain evaluated as the sum of shrinkage strain and thermal contraction strain deducted by 100 micro-strain as stipulated in BS 8007 (BSI, 1987). For type 2 deformed bars, the ratio (f_{ct}/f_b) may be taken as 0·67.

From the above, the following important characteristics of the method are noted.

- It is assumed that full bond strength would be developed along the steel bar–concrete interface. However, as can be seen from Figure 2, for ribbed bars, this is generally not possible unless the bond slip is larger than 0·6 mm or, in other words, the crack width is larger than 1·2 mm. Such an assumption would lead to overestimation of the bond stress and underestimation of the crack spacing.
- The predicted crack spacing is independent of the effective strain.
- The predicted crack width increases with the effective strain.

Model proposed by Nejadi and Gilbert

According to the model of Nejadi and Gilbert (2004), the concrete stress varies from zero at the crack to σ_{c1} at a distance of l_0 from the crack and then remains constant at further distance from the crack. On the other hand, the steel stress varies from σ_{s2} at the crack to σ_{s1} at a distance of l_0 from the crack and then remains constant at further distance from the crack. At the first crack, l_0 may be evaluated as $l_0 = \phi/(10\rho)$, but at the final or long-term stage, the value of l_0 should be multiplied by 1·33 to become $\phi/(7{\cdot}5\rho)$ so as to cater for the deterioration

in bond with time. The distance l_0 may be interpreted as the minimum crack spacing.

After first cracking, the concrete stress σ_{c1} at distance l_0 from the crack and the steel stress σ_{s2} at the crack are derived as follows (Gilbert, 1992, 2001, 2003)

$$7. \quad \sigma_{c1} = \frac{(3L)m\rho f_{ct}}{2l_0 + (3L)m\rho}$$

$$8. \quad \sigma_{s2} = \frac{(3L - 2l_0)mf_{ct}}{2l_0 + (3L)m\rho}$$

where L is the length of the concrete member between restraints, m is the modular ratio (E_s/E_c) and ρ is the steel ratio (A_s/A_c). After all shrinkage has taken place and the final crack pattern is established, the final concrete stress at distance l_0 from a crack (σ^*_{c1}) and the final steel stress at each crack (σ^*_{s2}) become

$$9. \quad \sigma^*_{c1} = \frac{3E_s\rho\Delta u}{2n_{cr}l_0} - \frac{(3L)m^*\rho}{2n_{cr}l_0}(\sigma_{av} + \varepsilon^*_{cs}E^*_c) \leq f_{ct}$$

$$10. \quad \sigma^*_{s2} = \frac{3E_s\Delta u}{2n_{cr}l_0} - \frac{(3L - 2n_{cr}l_0)m^*}{2n_{cr}l_0}(\sigma_{av} + \varepsilon^*_{cs}E^*_c)$$

in which Δu is the change in length of the member due to support movement, n_{cr} is the number of cracks, σ_{av} is the average stress in the uncracked concrete, ε^*_{cs} is the ultimate concrete shrinkage strain, E^*_c is the effective elastic modulus of concrete and m^* is the effective modular ratio (E_s/E^*_c). The average concrete stress σ_{av} may be taken as $(\sigma_{c1} + f_{ct})/2$ in which f_{ct} is the concrete tensile strength, whereas the effective elastic modulus E^*_c may be taken as $E_c/(1 + \phi^*_c)$ in which ϕ^*_c is the final creep coefficient. On the other hand, the number of cracks n_{cr} should be taken as the smallest integer value such that $\sigma^*_{c1} \leq f_{ct}$. Lastly, provided the steel at the crack has not yielded, the final mean crack width w is given by

$$11. \quad w = -\left[\frac{\sigma^*_{c1}}{E^*_c}\left(\frac{L}{n_{cr}} - \frac{2}{3}l_0\right) + \varepsilon^*_{cs}\left(\frac{L}{n_{cr}}\right)\right]$$

The following important characteristics of the model are noted.

- The actual bond stress distribution is not evaluated as a part of the solution.
- The minimum crack spacing is dependent only on the steel bar diameter and ratio.
- The number of cracks increases, whereas the mean crack spacing decreases as the magnitude of shrinkage strain increases.
- The predicted mean crack width w increases with the magnitude of shrinkage strain.

Model proposed by Häußler-Combe and Hartig

Like the other models, the model developed by Häußler-Combe and Hartig (2012) assumes that there is a certain bond force transfer length at the two sides of a crack, within which the bond force at the steel bar–concrete interface would cause the concrete stresses to vary from zero at the crack to a maximum value at the end of the bond force transfer length and the steel stress, to vary from a maximum value at the crack to a minimum value at the end of the bond force transfer length.

According to this model, the crack width w of a symmetrical crack can be calculated as

$$12. \quad w = 2l_t(\varepsilon_{sm} - \varepsilon_{cm})$$

where l_t is the bond force transfer length, ε_{sm} is the mean strain of the steel and ε_{cm} is the mean strain of the concrete. In turn, the mean strains are evaluated from the corresponding mean stresses. Let the maximum steel stress be σ_{sr} and the change in steel stress between the two ends of the transfer length be $\Delta\sigma_s$. The mean steel stress σ_{sm} may be evaluated as

$$13. \quad \sigma_{sm} = \sigma_{sr} - \beta_t\Delta\sigma_s$$

where β_t is a constant empirical factor describing the shape of the stress distribution in the steel along the transfer length. Likewise, the mean concrete stress σ_{cm} may be evaluated as

$$14. \quad \sigma_{cm} = \rho\beta_t\Delta\sigma_s$$

in which $\rho = A_s/A_c$ is the steel ratio. The force transfer between the steel bar and concrete is effected by the bond stresses developed along the transfer length. Based on equilibrium

$$15. \quad \Delta\sigma_s = \frac{n\pi\phi}{A_s}l_t\tau_m = \left(\frac{4}{\phi}\right)l_t\tau_m$$

where n is the number of steel bars and τ_m is the mean bond stress. For simplicity, it is assumed that $\tau_m = \gamma f_{ct}$, where γ is a proportionality constant and f_{ct} is the concrete tensile strength. Since the concrete stress increases from zero at the crack to a maximum value of $\rho\Delta\sigma_s$ at the end of the transfer length, and the concrete stress cannot be larger than f_{ct}, $\Delta\sigma_s$ has a maximum value of f_{ct}/ρ. As a result, the transfer length l_t is subjected to an upper limit of l^*_t, which can be determined by substituting $\Delta\sigma_s = f_{ct}/\rho$ into Equation 15, giving

$$16. \quad l^*_t = \left(\frac{\phi}{4\rho}\right)\left(\frac{f_{ct}}{\tau_m}\right)$$

Let the crack spacing be s_r. The crack spacing s_r cannot be longer than $2l_t^*$ because otherwise the maximum concrete stress ($=\rho\Delta\sigma_s$) occurring at the mid-point between two adjacent cracks would exceed the concrete tensile strength and a new crack would be formed. Hence, the crack spacing s_r has to satisfy the condition

17. $$l_t^* \le s_r \le 2l_t^*$$

In other words, there is a maximum crack spacing of $2l_t^*$ and a minimum crack spacing of l_t^*.

For a RC member subjected to an imposed strain $\varepsilon_{cE} < 0$ over the entire length L (the imposed strain could be shrinkage or thermal contraction strain) and having a total of n_{cr} cracks formed in the stabilised cracking state, the mean crack width w may be evaluated from Equation 18 based on the compatibility condition

18. $$n_{cr}w + \left(L\varepsilon_{cE} + \frac{n_{cr}(2l_t)\sigma_{cm}}{E_c}\right) = \Delta u$$

in which Δu is the change in length of the member due to support movement. Substituting the value of $\sigma_{cm} = \rho\beta_t\Delta\sigma_s$ and the value of $l_t = (\phi/4)(\Delta\sigma_s/\tau_m)$ into the above equation and assuming that $\Delta\sigma_s$ has its maximum value of f_{ct}/ρ, the formula for the mean crack width w under the condition of stabilised cracking is derived as

19. $$w = \left(\frac{\phi}{2\rho}\right)\left(\frac{f_{ct}}{\tau_m}\right)\left(\frac{\Delta u}{L} - \varepsilon_{cE} - \beta_t\frac{f_{ct}}{E_c}\right)$$

in which E_c is the effective elastic modulus of concrete. To account for creep, the effective elastic modulus may be taken as the elastic modulus divided by the factor $(1 + \phi_c)$, where ϕ_c is the creep coefficient.

This model has the following characteristics.

- The actual bond stress distribution is not evaluated as a part of the solution.
- The computed results are dependent on the assumed values of the coefficients β_t and γ.
- Both the minimum crack spacing l_t^* and maximum crack spacing $2l_t^*$ are independent of the shrinkage strain.
- The computed mean crack width w increases with the magnitude of shrinkage strain.

A new and rigorous analytical model

The existing methods of shrinkage cracking analysis detailed in the previous section differ widely in their formulations and are therefore not consistent with each other. Actually, none of the methods are capable of giving the actual variations of the bond, concrete and steel stresses along the RC member. The previous models generally assume that there is a well-defined bond force transfer length at each side of the crack and that the bond stress varies within the transfer length with a certain fixed mean bond stress. The authors of this paper do not agree with these assumptions and are of the view that evaluation of the actual variations of the bond, concrete and steel stresses should be incorporated as an integral part of the formulation, as presented below.

In the following, a RC member subjected to a shrinkage strain of ε_{cs} and an imposed strain of $\Delta u/L$ due to support movement (Δu is the change in length and L is the total length) is analysed. If only one crack has formed, the segment of the member from the crack to one end of the member is considered. If two or more cracks have formed, the segment of the member from one crack to the mid-point between this crack and the adjacent crack is considered. The segment under consideration here is shown in Figure 3. The maximum bond slip ξ occurs at the crack; at the end of the segment, the bond slip is equal to zero because of symmetry or end fixity. Let the distance from the crack be x and the displacements of concrete and steel be u_c and u_s, respectively. These displacements are related to the concrete stress σ_c, steel stress σ_s and bond stress τ_b by the equations

20. $$\frac{\partial u_c}{\partial x} = \varepsilon_{cs} + \frac{\sigma_c}{E_c}$$

21. $$\frac{\partial u_s}{\partial x} = \frac{\sigma_s}{E_s}$$

22. $$u_c - u_s = \frac{\tau_b}{k_b}$$

in which E_c is the elastic modulus of concrete, E_s is the elastic modulus of steel and k_b is the bond stiffness. The equilibrium condition gives rise to

23. $$n\pi\phi\tau_b = A_c\frac{\partial\sigma_c}{\partial x} = -A_s\frac{\partial\sigma_s}{\partial x}$$

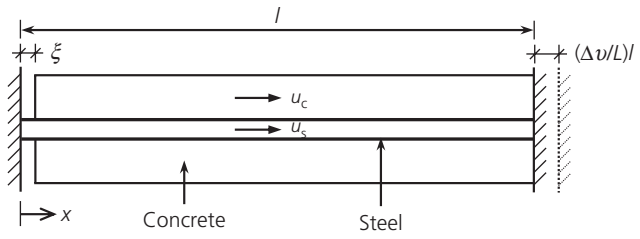

Figure 3. Segment of RC member subjected to shrinkage

where n is the number of steel bars, ϕ is the steel bar diameter, A_c is the concrete area and A_s is the steel area. Expressing in terms of displacements only, the following differential equation is obtained

$$24. \quad n\pi\phi k_b(u_c - u_s) = E_c A_c \frac{\partial^2 u_c}{\partial x^2} = -E_s A_s \frac{\partial^2 u_s}{\partial x^2}$$

Dividing the whole equation by $E_c A_c$ and introducing the parameter λ, which denotes the ratio

$$25. \quad \lambda = \frac{n\pi\phi k_b}{E_c A_c} = \left(\frac{4\rho}{\phi}\right)\left(\frac{k_b}{E_c}\right)$$

Equation 24 becomes

$$26. \quad \lambda(u_c - u_s) = \frac{\partial^2 u_c}{\partial x^2} = -m\rho \frac{\partial^2 u_s}{\partial x^2}$$

in which m is the modular ratio (E_s/E_c) and ρ is the steel ratio (A_s/A_c).

Equation 26 is the governing equation of the structural system. It is actually a set of two second-order partial differential equations, which need to be solved with the boundary conditions considered. The boundary conditions are

- at the crack: $x = 0$, $u_c = \xi$, $u_s = 0$ and $\sigma_c = 0$
- at the end of the segment: $x = l$, $u_c = (\Delta u/L)l$, $u_s = (\Delta u/L)l$ and $\sigma_c \leq f_{ct}$.

Note that l is the bond force transfer length from the crack (where the bond slip is maximum) to the end of the segment (where the bond slip is equal to zero). For conciseness, the procedures of solving the governing equation together with the boundary conditions are presented in the Appendix.

As explained in the Appendix, a parameter ψ is employed to solve the differential equations; ψ is defined as

$$27. \quad \psi = \sqrt{\frac{\lambda(1+m\rho)}{m\rho}}$$

Solving the governing equation, the concrete stress in terms of the maximum bond slip ξ at the crack is obtained as

$$28. \quad \sigma_c(x) = E_c\left(\frac{\Delta u}{L} - \varepsilon_{cs} - \xi \cdot \frac{m\rho\psi}{1+m\rho} \cdot \frac{\cosh(\psi(l-x))}{\sinh(\psi l)} - \xi \cdot \frac{1/l}{1+m\rho}\right)$$

At $x = 0$, $\sigma_c = 0$. This boundary condition yields

$$29. \quad \frac{\Delta u}{L} - \varepsilon_{cs} - \xi \cdot \frac{m\rho\psi}{1+m\rho} \cdot \frac{\cosh(\psi l)}{\sinh(\psi l)} - \xi \cdot \frac{1/l}{1+m\rho} = 0$$

Solving Equation 29, the maximum bond slip ξ is obtained as

$$30. \quad \xi = \frac{1+m\rho}{1+(m\rho\psi l/\tanh(\psi l))}\left(\frac{\Delta u}{L} - \varepsilon_{cs}\right) l$$

Substituting into Equation 28, the concrete stress in terms of the shrinkage strain ε_{cs} is obtained as

$$31. \quad \sigma_c(x) = E_c\left(\frac{\Delta u}{L} - \varepsilon_{cs}\right)\left(\frac{m\rho\psi l}{m\rho\psi l + \tanh(\psi l)}\right) \times \left(1 - \frac{\cosh(\psi(l-x))}{\cosh(\psi l)}\right)$$

The variations of the concrete stress σ_c with the distance x from the crack for some typical cases (i.e. the specimens analysed in next section) are illustrated in Figure 4. The maximum concrete stress occurs at $x = l$ and is derived from Equation 31 as

$$32. \quad \sigma_c(l) = E_c\left(\frac{\Delta u}{L} - \varepsilon_{cs}\right)\left(\frac{m\rho\psi l}{m\rho\psi l + \tanh(\psi l)}\right)\left(1 - \frac{1}{\cosh(\psi l)}\right)$$

Since the maximum concrete stress cannot be larger than the concrete tensile strength, the following inequality applies

$$33. \quad E_c\left(\frac{\Delta u}{L} - \varepsilon_{cs}\right)\left(\frac{m\rho\psi l}{m\rho\psi l + \tanh(\psi l)}\right)\left(1 - \frac{1}{\cosh(\psi l)}\right) \leq f_{ct}$$

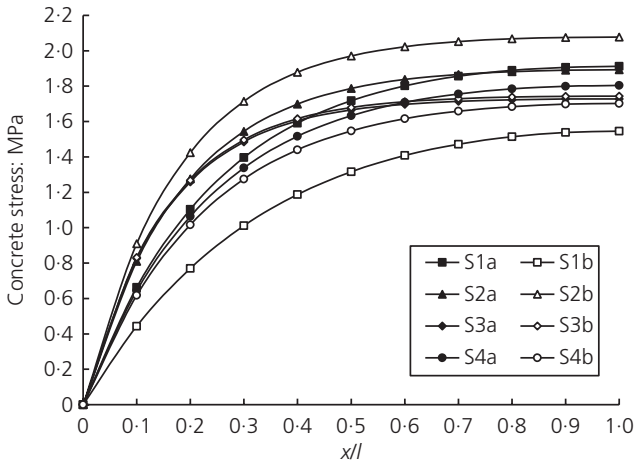

Figure 4. Variations of concrete stress with distance from a crack

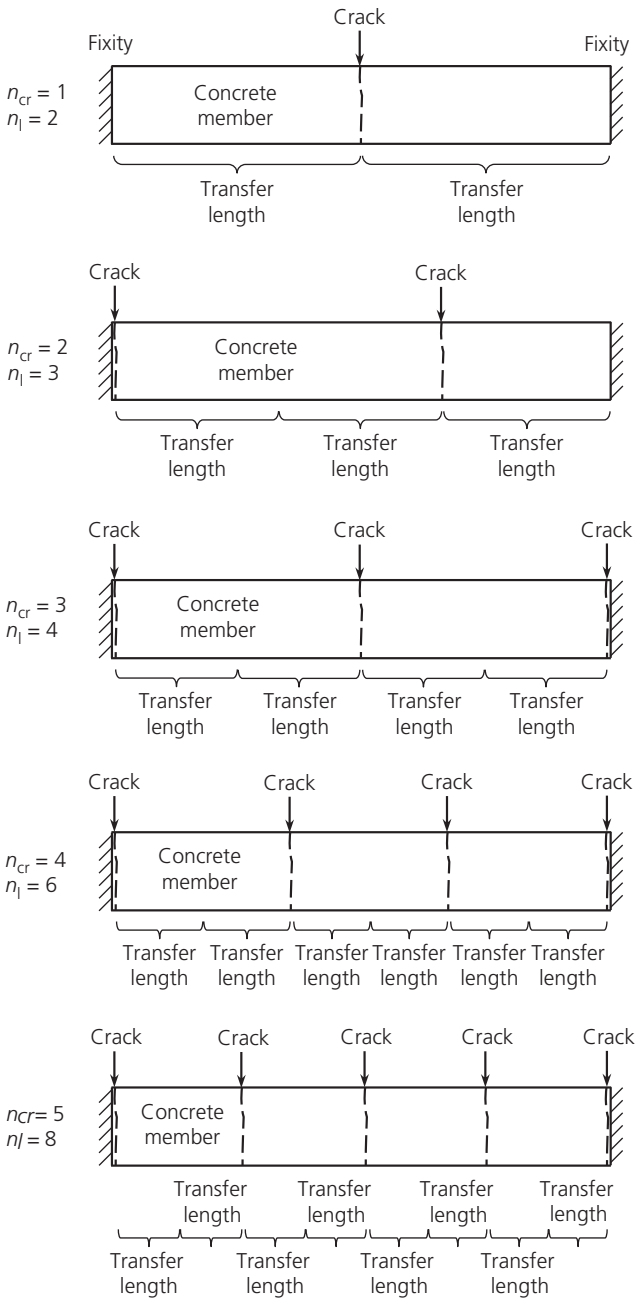

Figure 5. Number of cracks and number of transfer lengths

From this inequality, the upper limit of l, denoted l^*, is obtained as

$$34. \quad l^* = \left(\frac{1}{m\rho\psi}\right)\left(\frac{\tanh(\psi l) f_{ct}}{E_c[(\Delta u/L) - \varepsilon_{cs}][1 - (1/\cosh(\psi l))] - f_{ct}}\right)$$

In most cases, $\psi l \geq 3{\cdot}0$, $\tanh(\psi l) \approx 1{\cdot}0$ and $1/\cosh(\psi l) < 0{\cdot}1$, and the exact value of ψl has little effect on the value of l^*. Adopting the arguments of Häußler-Combe and Hartig (2012), the crack spacing s_r has to satisfy the condition

$$35. \quad l^* \leq s_r \leq 2l^*$$

Hence, the crack spacing s_r could vary between l^* and $2l^*$ and the transfer length l, which is equal to half the crack spacing, could vary between $0{\cdot}5l^*$ and l^*.

The crack width is related to the crack spacing and the transfer length. However, the crack spacing is sometimes undefined but the transfer length is always well defined, as illustrated in Figure 5. For instance, when there is only one crack within the length of the member, the crack spacing is undefined but there will be two transfer lengths with a mean transfer length equal to half the length of the member. When there is one crack within the length and another crack at one end of the member, there is only one crack spacing between the two cracks and the mean crack spacing is difficult to define, whereas there will be three transfer lengths with a mean transfer length of one-third the length of the member. In fact, the crack width is related more to the transfer length than the crack spacing. From Equation 30, it can be seen that the maximum bond slip ξ is directly related to the transfer length l, not the crack spacing s_r. For a crack within the length of the member, the crack width is equal to 2ξ because there are bond slips of concrete away from the crack at both sides, whereas for a crack at the end of the member, the crack width is equal to ξ because there is bond slip of concrete away from the crack at only one side.

It is thus suggested that we should work with the transfer length, rather than the crack spacing. Let the number of cracks be n_{cr}. Each crack within the length of the member would produce two transfer lengths, while each crack at the end of the member would produce only one transfer length. Assuming that the first crack would be formed within the length, the second crack would be formed at one end, the third crack would be formed at the other end and subsequent cracks would be formed within the length again, the number of transfer lengths n_l may be determined as

$$36. \quad n_l = 2n_{cr} - \min(n_{cr} - 1, 2)$$

From the number of transfer lengths n_l so determined, the mean transfer length l may be evaluated as

$$37. \quad l = \frac{L}{n_l} = \frac{L}{2n_{cr} - \min(n_{cr} - 1, 2)}$$

The actual number of cracks n_{cr} should be taken as the smallest integer value such that the mean transfer length l

evaluated using Equation 37 satisfies the condition $l \leq l^*$ (so as to ensure that the maximum concrete stress $\sigma_c(l)$ is not larger than the concrete tensile strength f_{ct}). Then, the mean transfer length l may be substituted into Equation 30 to evaluate the mean value of ξ. With the mean value of ξ so evaluated, the total crack width may be calculated as the number of transfer lengths n_l times the mean value of ξ. Finally, the mean crack width w may be evaluated as the total crack width divided by the number of cracks, or simply as $(n_l/n_{cr})\xi$. Multiplying Equation 30 by n_l/n_{cr}, the mean crack width w is obtained as

$$38. \quad w = \frac{1 + m\rho}{1 + (m\rho\psi l/\tanh(\psi l))}\left(\frac{\Delta u}{L} - \varepsilon_{cs}\right)\left(\frac{L}{n_{cr}}\right)$$

Having completed the formulation, it is noted that the analytical solutions derived above are closed-form in nature and are not dependent on any assumed empirical coefficients.

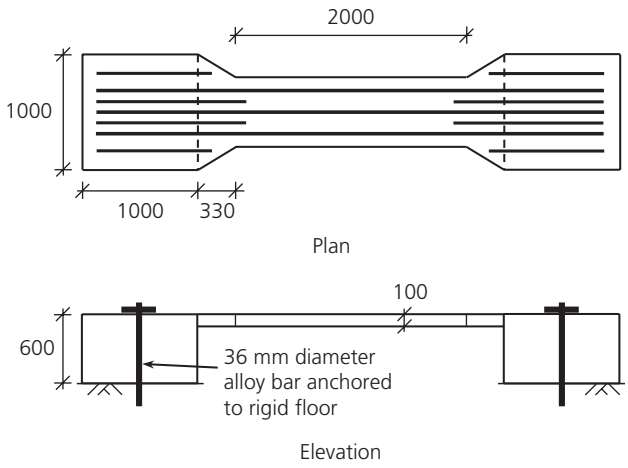

Figure 6. Details of concrete slab specimens tested by Nejadi and Gilbert (2004); dimensions in mm

Analysis of test specimens

To validate the new analytical model, the RC slab specimens tested by Nejadi and Gilbert (2004) were analysed. The dimensions and details of the specimens are shown in Figure 6 and listed in Table 1. Each specimen consisted of a 600 mm wide by 2000 mm long prismatic portion connected monolithically via two 330 mm long splayed portions to end blocks of 1·0 m by 1·0 m by 0·6 m depth at the ends. The end blocks were firmly clamped to a rigid floor to provide effective restraints to the shrinkage movement of the prismatic portion. The splayed portions, having the same depth, were to avoid stress concentration. A total of eight specimens reinforced with two to four steel bars of 10–12 mm diameter were tested. At the mid-length of each specimen, two 75 mm wide full-depth notches were formed at the two sides during concrete casting to induce the first crack there.

The eight specimens were cast from two batches of concrete. The material properties of each batch of concrete (compressive strength, tensile strength, elastic modulus, shrinkage strain and creep coefficient) as reported by Nejadi and Gilbert (2004) are presented in Table 2. The specimens were kept undisturbed and the number of cracks, the crack spacing, crack width and steel strain of each specimen were measured. Furthermore, due to shrinkage and fixity of the end blocks, the prismatic portion of each specimen was elongated and the elongation of each specimen was measured. The elongation, number of cracks, mean crack spacing and crack width, and maximum steel and concrete stresses (derived from the measured steel strains) as reported by Nejadi and Gilbert (2004), are listed in Table 3.

These specimens were also analysed by Nejadi and Gilbert (2004) and by Häußler-Combe and Hartig (2012) using their own analytical models. The respective analysis results are summarised in Tables 4 and 5 (note that in both tables, the number of cracks includes the artificially induced crack at the middle). It can be seen that both models predict that specimens S1a and S1b should have the largest number of cracks and the smallest mean crack width, whereas specimens S3a

Specimen	Concrete	Number of steel bars, n	Steel bar diameter, ϕ: mm	Steel area, A_s: mm^2	Concrete depth: mm
S1a	Batch I	3	12	339	102·2
S1b	Batch I	3	12	339	99·8
S2a	Batch I	3	10	236	101·6
S2b	Batch II	3	10	236	98·3
S3a	Batch I	2	10	157	99·2
S3b	Batch I	2	10	157	99·3
S4a	Batch I	4	10	314	100·5
S4b	Batch I	4	10	314	101·1

Table 1. Dimensions and details of specimens tested by Nejadi and Gilbert (2004)

and S3b should have the smallest number of cracks and the largest mean crack width. These predictions agree fairly well with the experimental results. However, the model of Nejadi and Gilbert (2004) predicts that the maximum steel stress in specimens S3a and S3b should be around 553–562 MPa, but the model of Häußler-Combe and Hartig (2012) predicts that the maximum steel stress in specimens S3a and S3b should be around 499–503 MPa. Moreover, the Nejadi and Gilbert (2004) model predicts that the maximum concrete stress should vary from 1·22 to 1·68 MPa but the Häußler-Combe and Hartig (2012) model predicts that the maximum concrete stress should remain constant at 1·97 MPa. The two models thus do not quite agree.

The specimens were also analysed using the new analytical model presented here. In conducting the analysis, the materials properties reported by Nejadi and Gilbert (2004) were used. Regarding the steel properties, the elastic modulus was assumed to be 200 GPa and the yield strength was assumed to be high enough to avoid yielding. The concrete was assumed to be linearly elastic, with its tensile strength and elastic modulus as given in Table 2. Regarding the bond properties, the bond stiffness k_b was taken as the mean secant stiffness evaluated using Equation 2. Since the mean secant stiffness is dependent on the maximum bond slip, it was determined by an iterative process. First, it was evaluated as that corresponding to a maximum bond slip of 0·15 mm. Then, it was used to conduct shrinkage cracking analysis, from which the maximum bond slip was obtained. The maximum bond slip so obtained was used to re-evaluate the mean secant stiffness so as to obtain an updated value. The updated mean secant stiffness was then used to conduct the shrinkage cracking analysis again, and the analysis was repeated. For all the specimens analysed, the mean secant stiffness converged rapidly and only two or three iterations were needed to obtain convergent results. The analytical results obtained by this new model are given in Table 6, where the mean transfer length instead of the mean crack spacing is presented.

Concrete material properties	Batch I	Batch II
Compressive strength at 28 d: MPa	24·3	28·4
Tensile strength at 28 d: MPa	1·97	2·10
Elastic modulus at 28 d: MPa	22 810	23 210
Shrinkage strain at 122 d: με	457	495
Creep coefficient at 122 d	0·98	1·16

Table 2. Concrete material properties of Nejadi and Gilbert (2004) test specimens

To facilitate the comparison, the experimental crack widths and crack widths from the three analytical models are listed together in Table 7. The table shows that there is a very large discrepancy between the experimental crack width of specimen S3a and the corresponding crack widths from all three analytical models. For specimen S3a, the experimental crack width of 0·84 mm appears to be exceptionally large, bearing in mind that the analytical crack widths obtained by the three models are all within 0·51 to 0·56 mm. The experimental results reveal that, for this particular specimen, there was only one crack in the middle and the maximum steel stress at the crack was as high as 532 MPa. Hence, there is a strong possibility that the steel bars in this specimen had yielded during cracking, thus causing the formation of a very wide crack. Particular care is therefore needed when interpreting the experimental results of specimen S3a.

For an assessment of accuracy, the percentage errors of the mean crack width predictions by the three analytical models were evaluated and these are also presented in Table 7. With all specimens included, the mean absolute errors of the mean crack width predictions by the models of Nejadi and Gilbert (2004) and Häußler-Combe and Hartig (2012) and the new model are 15·6%, 19·1% and 13·7%, respectively. With specimen S3a excluded, the mean absolute errors are 12·3%, 16·8%

Specimen	Elongation, Δu: mm	Number of cracks	Mean crack spacing: mm	Mean crack width: mm	Maximum steel stress: MPa	Maximum concrete stress: MPa
S1a	0·305	4	670	0·21	273	1·77
S1b	0·383	4	403	0·18	190	1·41
S2a	0·309	3	674	0·30	250	1·13
S2b	0·315	3	700	0·31	290	1·46
S3a	0·402	1	Undefined	0·84	532	1·45
S3b	0·419	2	997	0·50	467	1·31
S4a	0·245	3	783	0·23	270	1·64
S4b	0·162	3	995	0·25	276	1·71

Table 3. Experimental results reported by Nejadi and Gilbert (2004)

Specimen	Number of cracks	Mean crack spacing: mm	Mean crack width: mm	Maximum steel stress: MPa	Maximum concrete stress: MPa
S1a	4	667	0·19	246	1·68
S1b	5	500	0·16	196	1·43
S2a	3	1000	0·28	337	1·54
S2b	4	667	0·26	235	1·22
S3a	1	Undefined	0·51	553	1·63
S3b	1	Undefined	0·50	562	1·65
S4a	4	667	0·18	261	1·66
S4b	4	667	0·20	227	1·47

Table 4. Analytical results reported by Nejadi and Gilbert (2004)

Specimen	Number of cracks	Mean crack spacing: mm	Mean crack width: mm	Maximum steel stress: MPa	Maximum concrete stress: MPa
S1a	5	500	0·25	275	1·97
S1b	5	500	0·26	289	1·97
S2a	4	667	0·33	369	1·97
S2b	—	—	—	—	—
S3a	3	1000	0·56	499	1·97
S3b	3	1000	0·56	503	1·97
S4a	5	500	0·23	295	1·97
S4b	5	500	0·21	279	1·97

Table 5. Analytical results reported by Häußler-Combe and Hartig (2012)

Specimen	Number of cracks	Mean transfer length: mm	Mean crack width: mm	Maximum steel stress: MPa	Maximum concrete stress: MPa
S1a	4	333	0·24	301	1·91
S1b	5	250	0·22	242	1·55
S2a	3	500	0·32	435	1·89
S2b	3	500	0·33	463	2·08
S3a	2	667	0·53	596	1·73
S3b	2	667	0·54	603	1·74
S4a	4	250	0·23	298	1·80
S4b	4	333	0·21	277	1·70

Table 6. Analytical results using the new analytical model

and 10·4%, respectively. Hence, based on the mean absolute errors, the new model has slightly better accuracy. Moreover, with specimen S3a excluded, the mean errors of the mean crack width predictions by the three models are −12·3%, +11·5% and +5·7%, respectively. Hence, the model of Nejadi and Gilbert (2004) tends to underestimate the mean crack width, the Häußler-Combe and Hartig (2012) model tends to overestimate the mean crack width, whereas the new model has insignificant tendency to either overestimate or underestimate the mean crack width (bearing in mind that the errors of predictions by the new model are partly due to experimental errors).

Conclusions

Existing analytical models for shrinkage cracking analysis of RC members have been reviewed and, in order to avoid reliance on

Specimen	w_{exp}: mm	Model of Nejadi and Gilbert (2004)		Model of Häußler-Combe and Hartig (2012)		New analytical model	
		w: mm	Error: %	*w*: mm	Error: %	*w*: mm	Error: %
S1a	0·21	0·19	−10	0·25	+19	0·24	+14
S1b	0·18	0·16	−11	0·26	+44	0·22	+22
S2a	0·30	0·28	−7	0·33	+10	0·32	+7
S2b	0·31	0·26	−16	Not analysed		0·33	+6
S3a	0·84	0·51	−39	0·56	−33	0·53	−37
S3b	0·50	0·50	0	0·56	+12	0·54	+8
S4a	0·23	0·18	−22	0·23	0	0·23	0
S4b	0·25	0·20	−20	0·21	−16	0·21	−16
Mean absolute error (with all specimens included): %			15·6		19·1		13·7
Mean absolute error (with S3a excluded): %			12·3		16·8		10·4
Mean error (with S3a excluded): %			−12·3		+11·5		+5·7

Table 7. Comparison of experimental (w_{exp}) and analytical mean crack widths (*w*)

empirical coefficients, a new and more rigorous analytical model was developed. The new model was formulated purely based on the mechanics of the steel bar–concrete interaction. From the formulation, two governing equations, which are second-order partial differential equations, were derived. With the bond stress–slip relation taken into account and the boundary conditions duly considered, the governing equations can be solved analytically without making any assumptions on the concrete, steel and bond stress distributions along the transfer length. In fact, the actual concrete, steel and bond stress distributions are evaluated as an integral part of the solution. The new model is therefore mathematically more rigorous than the existing models. Moreover, closed-form solutions are obtained, from which the effects of various parameters on the crack spacing and crack width may be evaluated algebraically, and the crack-control steel designed to meet the crack width requirements.

Apart from giving closed-form solutions, the new model has the unique feature that it works with the transfer length, rather than the crack spacing, which is sometimes undefined. Nevertheless, as with the existing models, it still considers the number of cracks. Basically, from the number of cracks, the number of transfer lengths is determined and the mean transfer length, which governs the maximum concrete stress, is evaluated. The number of cracks is taken as the smallest integer value such that the mean transfer length is not larger than the upper limit of the transfer length or the maximum concrete stress is not larger than the concrete tensile strength.

For validation and comparison with the existing models, the new model was applied to analyse eight specimens tested by Nejadi and Gilbert (2004). Due to randomness of cracking, there are occasionally significant errors in the predicted crack numbers and crack widths. Nevertheless, based on the absolute errors, the new model has slightly better accuracy in crack width prediction than the existing models. Moreover, based on the mean errors, the new model has the smallest tendency to over- or underestimate the crack width. Lastly, it is emphasised that the new model, which does not rely on any assumed values of empirical coefficients, should be more generally applicable. However, the theoretical predictions by the new model have been compared with only a limited number of experimental results and comparison with more experimental results for further verification is recommended.

Appendix: Solving the governing equations of concrete cracking

The governing equation (Equation 26) may be split into the following two equations

$$39. \quad \frac{\partial^2 u_c}{\partial x^2} = -m\rho \frac{\partial^2 u_s}{\partial x^2}$$

$$40. \quad \frac{\partial^2 u_c}{\partial x^2} = \lambda(u_c - u_s)$$

The solution procedures start with the following general solutions, in which ψ_1 and ψ_2 are the roots of the characteristic equation, and A, B, C and D and $\underline{A}$, $\underline{B}$, $\underline{C}$ and $\underline{D}$ are coefficients to be determined from the boundary conditions.

$$41. \quad u_c = A e^{\psi_1 x} + B e^{\psi_2 x} + Cx + D$$

42. $$u_s = \underline{A}e^{\psi_1 x} + \underline{B}e^{\psi_2 x} + \underline{C}x + \underline{D}$$

Substituting into Equations 39 and 40, the following equations are obtained

43.
$$A = -m\rho\underline{A}$$
$$B = -m\rho\underline{B}$$
$$C = \underline{C}$$
$$D = \underline{D}$$

44.
$$\psi_1^2 = \frac{\lambda(1+m\rho)}{m\rho}$$
$$\psi_2^2 = \frac{\lambda(1+m\rho)}{m\rho}$$

The characteristic equation (Equation 44) has two roots, ψ_1 and ψ_2. Let the parameter ψ be defined by

45. $$\psi = \sqrt{\frac{\lambda(1+m\rho)}{m\rho}}$$

The two roots of the characteristic equation are given by

46. $$\psi_1 = \psi$$

47. $$\psi_2 = -\psi$$

Substituting into Equations 41 and 42, the displacement functions are obtained as

48. $$u_c = -m\rho\underline{A}e^{\psi_1 x} - m\rho\underline{B}e^{\psi_2 x} + \underline{C}x + \underline{D}$$

49. $$u_s = \underline{A}e^{\psi_1 x} + \underline{B}e^{\psi_2 x} + \underline{C}x + \underline{D}$$

The boundary conditions that $u_c(0) = \xi$ and $u_s(0) = 0$ at $x = 0$ lead to

50. $$u_c(0) = -m\rho\underline{A} - m\rho\underline{B} + \underline{D} = \xi$$

51. $$u_s(0) = \underline{A} + \underline{B} + \underline{D} = 0$$

Likewise, the boundary conditions that $u_c(l) = (\Delta u/L)l$ and $u_s(l) = (\Delta u/L)l$ at $x = l$ lead to

52. $$u_c(l) = -m\rho\underline{A}e^{\psi_1 l} - m\rho\underline{B}e^{\psi_2 l} + \underline{C}l + \underline{D} = (\Delta u/L)l$$

53. $$u_s(l) = \underline{A}e^{\psi_1 l} + \underline{B}e^{\psi_2 l} + \underline{C}l + \underline{D} = (\Delta u/L)l$$

Solving Equations 50–53 yields

54. $$\underline{A} = \frac{\xi}{1+m\rho} \cdot \frac{e^{\psi_2 l}}{e^{\psi_1 l} - e^{\psi_2 l}}$$

55. $$\underline{B} = \frac{-\xi}{1+m\rho} \cdot \frac{e^{\psi_1 l}}{e^{\psi_1 l} - e^{\psi_2 l}}$$

56. $$\underline{C} = \frac{\Delta u}{L} - \frac{\xi/l}{1+m\rho}$$

57. $$\underline{D} = \frac{\xi}{1+m\rho}$$

Substituting into Equations 48 and 49 then yields

58. $$u_c = \frac{\Delta u}{L}x + \frac{\xi}{1+m\rho}\left(-m\rho\frac{e^{\psi_2 l}e^{\psi_1 x} - e^{\psi_1 l}e^{\psi_2 x}}{e^{\psi_1 l} - e^{\psi_2 l}} - \frac{x}{l} + 1\right)$$

59. $$u_s = \frac{\Delta u}{L}x + \frac{\xi}{1+m\rho}\left(\frac{e^{\psi_2 l}e^{\psi_1 x} - e^{\psi_1 l}e^{\psi_2 x}}{e^{\psi_1 l} - e^{\psi_2 l}} - \frac{x}{l} + 1\right)$$

From the above displacement functions, the concrete and steel stresses are obtained as

60. $$\sigma_c(x) = E_c\left(\frac{\Delta u}{L} - \varepsilon_{cs} - \xi \cdot \frac{m\rho\psi}{1+m\rho} \cdot \frac{\cosh(\psi(l-x))}{\sinh(\psi l)} - \xi \cdot \frac{1/l}{1+m\rho}\right)$$

61. $$\sigma_s(x) = E_s\left(\frac{\Delta u}{L} + \xi \cdot \frac{\psi}{1+m\rho} \cdot \frac{\cosh(\psi(l-x))}{\sinh(\psi l)} - \xi \cdot \frac{1/l}{1+m\rho}\right)$$

REFERENCES

BSI (1987) BS 8007:1987: Code of practice for design of concrete structures for retaining aqueous liquids. BSI, London, UK.

Castel A and Gilbert RI (2014) Influence of time-dependent effects on the crack spacing in reinforced concrete beams. *Structural Concrete* **15(3)**: 373–379.

CEB (Comité Euro-International du Béton) (1993) *CEB-FIP Model Code 1990: Model Code for Concrete Structures*. Thomas Telford, London, UK.

Gilbert RI (1992) Shrinkage cracking in fully restrained concrete members. *ACI Structural Journal* **89(2)**: 141–149.

Gilbert RI (2001) Shrinkage, cracking and deflection – the serviceability of concrete structures. *Electronic Journal of Structural Engineering* **1**: 15–37.

Gilbert RI (2003) Shrinkage cracking and crack control in fully-restrained reinforced concrete members. In *System-based Vision for Strategic and Creative Design: Proceedings of the Second International Conference on Structural and Construction Engineering, Rome, Italy* (Bontempi F (ed.)). Swets and Zeitlinger, Lisse, the Netherlands, pp. 1921–1927.

Gilbert RI and Ranzi G (2011) *Time-Dependent Behaviour of Concrete Structures*. Spon Press, Abingdon, UK.

Häußler-Combe U and Hartig J (2012) Evaluation of concrete cracking due to restrained thermal loading and shrinkage. *ACI Structural Journal* **109(1)**: 41–51.

Hughes BP (1971a) *Control of Thermal and Shrinkage Cracking in Restrained Reinforced Concrete Walls*. Construction Industry Research and Information Association, London, UK, CIRIA Technical Note 21.

Hughes BP (1971b) *Elimination of Shrinkage and Thermal Cracking in a Water-Retaining Structure*. Construction Industry Research and Information Association, London, UK, CIRIA Technical Note 36.

Jurkiewiez B, Destrebecq JF and Vergne A (1999) Incremental analysis of time-dependent effects in composite structures. *Computers and Structures* **73(1–5)**: 425–435.

Kwan AKH and Ng PL (2009) Shrinkage movement analysis of reinforced concrete floors constructed in stages. *Computers and Concrete* **6(2)**: 167–185.

Kwan AKH and Ng PL (2015) Remnant creep based visco-elastic model for concrete creep analysis. *Proceedings of the Institution of Civil Engineers – Structures and Buildings* **168(1)**: 3–14, http://dx.doi.org/10.1680/stbu.13.00028.

Kwan AKH, Au FTK and Lee PKK (2002) Minimizing shrinkage cracks in concrete structures for better serviceability and durability. *Proceedings of Innovative Buildings Symposium, Hong Kong*. The Hong Kong Institution of Engineers, Hong Kong, China, pp. 117–136.

Kwan AKH, Au FTK and Lee PKK (2003) High-performance concrete buildings for the new millennium. *Progress in Structural Engineering and Materials* **5(4)**: 263–273.

Kwan AKH, Au FTK, Wong HHC and Ng PL (2010) Shrinkage of Hong Kong granite aggregate concrete. *Magazine of Concrete Research* **62(2)**: 115–126, http://dx.doi.org/10.1680/macr.2008.62.2.115.

Liu CH, Au FTK and Lee PKK (2006) Estimation of shrinkage effects on reinforced concrete podiums. *HKIE Transactions* **13(4)**: 33–43.

Ma FJ and Kwan AKH (2015) Crack width analysis of reinforced concrete members under flexure by finite element method and crack queuing algorithm. *Engineering Structures* **105**: 209–219.

Nejadi S and Gilbert RI (2004) Shrinkage cracking and crack control in restrained reinforced concrete members. *ACI Structural Journal* **101(6)**: 840–845.

Neville AM (1955) Theories of creep in concrete. *ACI Journal* **52(9)**: 47–60.

Neville AM (1958) The influence of cement on creep of concrete and mortar. *PCI Journal* **2(1)**: 12–18.

Neville AM (2011) *Properties of Concrete*, 5th edn. Pearson, Harlow, UK.

Powers TC (1968) Mechanisms of shrinkage and reversible creep of hardened Portland cement paste. *Proceedings of International Conference on the Structure of Concrete, London, UK*. Cement and Concrete Association, Slough, UK, pp. 319–344.

Vandamme M and Ulm FJ (2009) Nanogranular origin of concrete creep. *Proceedings of the National Academy of Sciences* **106(26)**: 10552–10557.

HOW CAN YOU CONTRIBUTE?

To discuss this paper, please submit up to 500 words to the editor at journals@ice.org.uk. Your contribution will be forwarded to the author(s) for a reply and, if considered appropriate by the editorial board, it will be published as a discussion in a future issue of the journal.